JPPIPA 11(11) (2025)

Jurnal Penelitian Pendidikan IPA

http://jppipa.unram.ac.id/index.php/jppipa/index

Modeling of Contaminant Transport Through Groundwater Flow Using Visual MODFLOW in the Kasin Sub-Watershed, Malang City

Alifa Fajriani Martius[1*], Emma Yuliani[1], Andre Primantyo Hendrawan[1], Very Dermawan[1]

[1] Water Resources Engineering Department, Faculty of Engineering, Universitas Brawijaya, Malang, Indonesia.

Received: August 21, 2025
Revised: October 25, 2025
Accepted: November 25, 2025
Published: November 30, 2025

Corresponding Author:
Alifa Fajriani Martius
alifajrianimartius@gmail.com

DOI: 10.29303/jppipa.v11i11.12615

Abstract: This study investigates groundwater flow and nitrate transport in the Kasin Sub-watershed, Malang City, using Visual MODFLOW integrated with the MT3DMS module. Hydrogeological and geoelectrical data, groundwater levels, and nitrate concentration measurements (110 ppm) were used as model inputs. A transient simulation over 3,600 days (±10 years) was conducted to analyze plume migration. The results show that groundwater flow follows topographic gradients, moving from upland recharge zones to lowland discharge zones, with an average velocity of 0.25–0.40 m/day. The nitrate plume migrated southward, extending ±600–700 m horizontally and reaching ±25 m in depth. High concentrations (>100 ppm) remained near the source, while concentrations decreased to 20–40 ppm at greater distances due to advection and dispersion. Vertical sections indicated plume penetration into deeper aquifers, influenced by hydraulic pressure differences between strata, while permeable sandy and pumice tuff layers facilitated migration and clay acted as aquitards. These findings highlight the persistent nature of nitrate contamination, the role of aquifer heterogeneity, and the vulnerability of groundwater in urban catchments. In conclusion, nitrate pollution poses long-term risks to groundwater quality, emphasizing the importance of monitoring networks, aquifer protection policies, and improved land-use management to mitigate further contamination.

Keywords: Aquifer vulnerability; Groundwater modeling; Kasin Sub-watershed; MT3DMS; Nitrate contamination; Visual MODFLOW

Introduction

Groundwater is a vital resource for urban, agricultural, and industrial water supply, especially in areas where surface water is scarce or unreliable (Foster, 2022; Mulyadi et al., 2022; Priyan, 2021). In Malang City, the Kasin Sub-Watershed (Sub-DAS Kasin), which is part of the Brantas Groundwater Basin (CAT Brantas), plays a crucial role in providing clean water. The Brantas Basin has been designated a national groundwater priority due to its large potential for raw water supply but is increasingly under pressure from overexploitation and contamination, especially from domestic and industrial waste (Ministry of Energy and Mineral Resources Regulation No. 2/2017; Bappenas, 2020).

The hydrogeological setting of the Kasin Sub-Watershed facilitates the infiltration of rainfall into both shallow and deep aquifers. However, this condition also increases the vulnerability of groundwater to contamination. Foster et al. (2022) highlighted that permeable soil layers allow surface contaminants to percolate rapidly into aquifers without sufficient natural filtration. In densely populated areas like Malang City,

How to Cite:
Martius, A. F., Yuliani, E., Hendrawan, A. P., Hendrawan, A. P., & Dermawan, V. (2025). Modeling of Contaminant Transport Through Groundwater Flow Using Visual MODFLOW in the Kasin Sub-Watershed, Malang City. *Jurnal Penelitian Pendidikan IPA*, *11*(11), 122–128. https://doi.org/10.29303/jppipa.v11i11.12615

the lack of proper domestic wastewater treatment systems—such as leaking or poorly constructed septic tanks—further increases the risk of aquifer contamination by nitrates, phosphates, and organic pollutants (Alam et al., 2024; Bijay-Singh et al., 2021; Kuroda et al., 2009; Rashmi et al., 2020).

This environmental degradation poses significant public health risks and economic consequences, particularly for low-income populations reliant on shallow groundwater. As part of CAT Brantas, the Kasin Sub-Watershed has been categorized as a vulnerable zone, requiring integrated and science-based groundwater management strategies (Geological Agency, 2019). One such approach is subsurface modeling to understand the dynamics of groundwater flow and contaminant migration.

Visual MODFLOW is a widely used groundwater modeling software that simulates flow and contaminant transport across time and space. When integrated with the MT3DMS module, it can simulate advection, dispersion, and chemical reactions of contaminants within aquifer systems (Jabeen et al., 2019; Samborska-Goik et al., 2024; Shakeri et al., 2023). By incorporating key hydrogeological parameters such as hydraulic conductivity, effective porosity, recharge rates, and contaminant properties, this study aims to model the contaminant transport in the Kasin Sub-Watershed. The goal is to provide scientific support for mitigation strategies and sustainable groundwater management in the region.

Method

This research was conducted in the Kasin Sub-Watershed area of Malang City, covering approximately 7.673 km², including parts of Klojen and Sukun Districts.

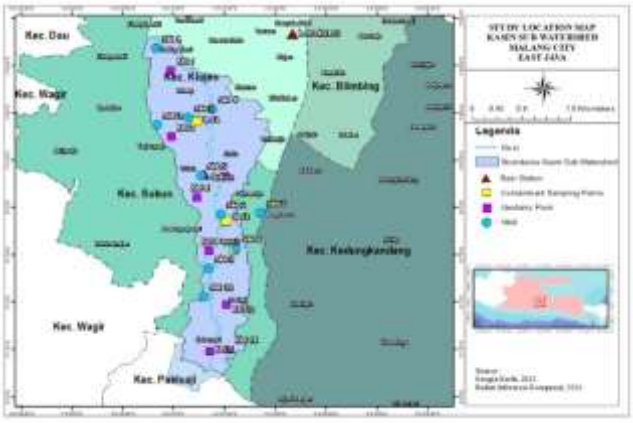

Figure 1. Study location map Kasin Sub-Watershed

MODFLOW solves the three-dimensional equation of groundwater flow, using a block-centered finite-difference approach (Laoufi et al., 2024).

$$\frac{\partial}{\partial x}\left(K_{xx}\frac{\partial h}{\partial x}\right)+\frac{\partial}{\partial y}\left(K_{yy}\frac{\partial h}{\partial y}\right)+\frac{\partial}{\partial z}\left(K_{zz}\frac{\partial h}{\partial z}\right)+W=S_s\frac{\partial h}{\partial t}$$

where *Kxx*, *Kyy*, and *Kzz* represent the values of hydraulic conductivity along the three orthogonal axes coordinates (*x*, *y* and *z*), h is the hydraulic head, *W* is the volumetric flow of sources/sinks, *Ss* is the specific storage, and *t* is time (Laoufi et al., 2024).

MT3DMS (Modular Three-Dimensional Multi-Species Transport Model) is a transport simulation module coupled with MODFLOW to model contaminant migration in groundwater systems (Zheng et al., 1999). It solves the advection–dispersion–reaction equation for solute transport in saturated porous media.

$$\frac{\partial(\theta C_k)}{\partial t}=\frac{\partial}{\partial x_i}\left(\theta D_{ij}\frac{\partial Ck}{\partial x_j}\right)-\frac{\partial}{\partial x_i}\left(\theta v_i C_k\right)+q_s\,C_{sk}+\sum R_n$$

Where, *Ck* is Concentration of dissolved species *k*, ML^{-3}; θ is Porosity of the subsurface medium, dimensionless *t* is Time, T; *xi* is Distance along each Cartesian coordinate axis, L; *Dij* is Tensor of hydrodynamic dispersion coefficients, L^2T^{-1}; *vi* is Seepage or pore-water linear velocity, LT^{-1}, related to specific discharge or Darcy flux through the relationship $vi = qi/\theta v$; *qs* is Volumetric flow rate per unit volume of aquifer representing source fluid (positive) and sink (negative), T^{-1}; *Csk* is Concentration of source or sink flux for species *k*, ML^{-3}; *ΣRn* is Chemical reaction term, $ML^{-3}T^{-1}$

The geoelectrical method in this study employed the Vertical Electrical Sounding (VES) technique with a Schlumberger configuration to obtain subsurface resistivity profiles. An electric current (I) was introduced through the current electrodes, while the potential difference (ΔV) was measured at the potential electrodes. The apparent resistivity was calculated using the equation $\rho_a = K\frac{\Delta V}{I}$ where *K* is the geometric factor determined by the electrode configuration. The apparent resistivity data were then processed through inversion using IPI2WIN software to derive the true resistivity, thickness, and depth of each subsurface layer (Eluwole et al., 2020; Eze et al., 2022; Ibrahim et al., 2025; Prayogo et al., 2024).

The geoelectrical method using the Schlumberger configuration is applied not only to determine subsurface resistivity and layer thickness but also to estimate hydrogeological parameters such as hydraulic conductivity, transmissivity, and porosity. Recent studies have demonstrated that subsurface resistivity, when integrated with layer thickness, can be used to map aquifer potential and estimate geo-hydraulic parameters. For example, Rasool et al. (2020) combined geoelectrical resistivity surveys with inversion modeling (IX1D) in Faisalabad, Pakistan, to derive layer resistivity and thickness, which were then used to calculate transmissivity and hydraulic conductivity as essential inputs for aquifer mapping and groundwater quality assessment. Similarly, Akiang et al. (2023) showed that

Schlumberger VES data could be correlated with aquifer parameters, allowing the estimation of transmissivity and hydraulic conductivity from geoelectrical sounding.

The procedure for applying to a groundwater flow model includes the following steps: Step 1, Sub-watershed delineation of Kasin Sub-DAS was performed using ArcGIS with a 30 m resolution DEM to define the spatial boundary of the model. Step 2, Aquifer characterization was derived from the interpretation of Vertical Electrical Sounding (VES) data at 8 measurement points, providing hydraulic conductivity (K) parameters as model input. Step 3, Groundwater level measurements from dug wells were used for model calibration, while rainfall data determined the recharge rate. Step 3, Grid construction with 250 m × 250 m cells and multiple vertical layers represented the aquifer stratigraphy. Step 4, Steady-state simulation was conducted for initial head distribution calibration, followed by a transient simulation over 3600 days (10 stress periods) to model groundwater flow dynamics. Step 5, Simulation of nitrate contaminant dispersion patterns with an initial concentration of 110ppm measured in the field.

Hydrogeological Characteristics

According to the legend of the Hydrogeological Map at a scale of 1:250,000, the Kasin Sub-watershed is composed of Quaternary volcanic deposits consisting of tuffaceous sandstone, volcanic breccia, and altered lava in the upland areas, while the middle to downstream zones are dominated by alluvial deposits of sand, gravel, and clay. The volcanic deposits are characterized by moderate to high permeability and are represented on the map by patterned blue or green areas, whereas the alluvial deposits with moderate permeability are shown as light green plain colors. This lithological variation governs the hydrogeological setting, where the volcanic uplands function as the main recharge zone and the alluvial plains act as discharge zones.

Figure 2 . Matching sub-watershed Kasin and hydrogeological maps

Groundwater systems in the Kasin Sub-watershed consist of both unconfined and confined aquifers. The unconfined aquifers are widely developed in the alluvial plains with relatively shallow water table depths (approximately 3–10 m), making them highly vulnerable to surface-derived contamination. Confined aquifers are found beneath intercalated clay layers, which act as aquitards limiting vertical flow and providing partial protection against contamination. Aquifer productivity ranges from moderate to high, with moderate productivity represented in green and high productivity in blue on the hydrogeological map. Groundwater flow direction, indicated by blue arrows, is oriented from the volcanic uplands towards the lower alluvial plains, consistent with the hydraulic gradient shown by water table contour lines. These findings highlight that the interplay between lithology, permeability, and aquifer productivity controls both the groundwater flow regime and the potential vulnerability of groundwater resources in the Kasin Sub-watershed.

Result and Discussion

Geophysical Measurement Results

The geoelectrical survey using the Vertical Electrical Sounding (VES) method at eight measurement points in the Kasin Sub-watershed revealed a sequence of five to six subsurface layers with varying thicknesses depending on the local morphology. The resistivity inversion identified the subsurface lithology as part of the Malang Tuff Formation, primarily composed of weathered volcanic material with fractures. The lithological units consist of top soil, clay, tuff, sandy tuff, pumice tuff, and breccia tuff.

Table 1. Geoelectrical Survey

Site	Depth (m)	Resistivity (Ωm)	Lithology
TGL 1 (Bareng, Klojen)	0–1.25	6.78	Top Soil
	1.25–2.14	4.6	Clay
	2.14–4.68	119	Pumice Tuff
	4.68–11.8	14.5	Clay
	11.8–50	285	Breccia Tuff
TGL 2 (Tanjungrejo, Sukun)	0–2.51	7.99	Top Soil
	2.51–3.87	79.3	Tuff
	3.87–5.25	3.4	Clay
	5.25–19.5	35.8	Tuff
	19.5–50	90.4	Pumice Tuff
TGL 3 (Kasin, Sukun)	0–1.50	115	Top Soil
	1.50–3.64	67.2	Sandy Tuff
	3.64–8.85	389	Breccia Tuff
	8.85–21.5	180	Pumice Tuff
	21.5–50	95.2	Pumice Tuff
TGL 4 (Sukun, Sukun)	0–1.25	7.12	Top Soil
	1.25–1.75	109	Pumice Tuff
	1.75–6.04	13.1	Clay

Site	Depth (m)	Resistivity (Ωm)	Lithology
	6.04–14.2	51.3	Sandy Tuff
	14.2–50	130	Pumice Tuff
TGL 5 (Bandungrejosari, Sukun)	0–1.25	11.5	Top Soil
	1.25–2.18	3.73	Clay
	2.18–5.38	43.4	Tuff
	5.38–13.6	8.28	Clay
	13.6–50	89.7	Pumice Tuff
TGL 6 (Gadang, Sukun)	0–2.28	6.94	Top Soil
	2.28–4.31	95.5	Pumice Tuff
	4.31–8.47	3.59	Clay
	8.47–25	196	Pumice Tuff
	25–50	79.3	Sandy Tuff
TGL 7 (Kebonsari, Sukun)	0–1.50	12.5	Top Soil
	1.50–4.51	9.27	Clay
	4.51–12.2	21.8	Tuff
	12.2–24.1	9.24	Clay
	24.1–50	195	Pumice Tuff
TGL 8 (Kebonsari, Sukun)	0–1.50	6.73	Top Soil
	1.50–3.83	40.3	Tuff
	3.83–10.3	18.9	Clay
	10.3–28.4	22.7	Tuff
	28.4–50	190	Pumice Tuff

The sandy tuff and pumice tuff layers exhibited relatively high resistivity values and were interpreted as productive aquifers, while clay layers showed low resistivity values and act as aquitards, restricting vertical groundwater flow. This configuration indicates that the groundwater system in the Kasin Sub-watershed is mainly controlled by lateral flow through permeable layers, whereas aquitard layers maintain groundwater table stability. The spatial variability in resistivity also highlights the heterogeneity of the subsurface, which influences groundwater distribution and its vulnerability to contamination.

Hydraulic Conductivity

The hydraulic conductivity test in the Kasin Sub-watershed revealed values ranging from 0.28 to 1.42 m/day. The highest values were observed in Bareng (1.42 m/day) and Gadang (1.21 m/day), dominated by sandy tuff and pumice tuff, which act as productive aquifers with high permeability. Moderate values were recorded in Tanjungrejo, Kasin, and Sukun (0.87–1.08 m/day), while the lowest values were found in Kebonsari (0.28–0.63 m/day), where the lithology consists of tuff interbedded with clay. This variability indicates the heterogeneity of the aquifer system in the Kasin Sub-watershed, where high-conductivity zones function as preferential flow pathways, while low-conductivity zones serve more as storage units and barriers to lateral groundwater movement.

Table 2. Hydraulic Conductivity Value

Location	Hydraulic Conductivity (m/day)
Bareng (TGL 1)	1.42
Tanjungrejo (TGL 2)	1.08
Kasin (TGL 3)	0.95
Sukun (TGL 4)	0.87
Bandungrejosari (TGL 5)	0.74
Gadang (TGL 6)	1.21
Kebonsari (TGL 7)	0.63
Kebonsari (TGL 8)	0.28

Well Data

The variability in groundwater levels also highlights differences in aquifer characteristics. Shallow wells tend to be more vulnerable to contamination due to their direct connectivity with the surface, while deeper wells are relatively protected by the presence of intercalated clay layers functioning as aquitards. Hydrogeologically, these findings emphasize the interplay between topography, lithology, and aquifer productivity in controlling groundwater conditions in the Kasin Sub-watershed.

Table 3. Groundwater Level Data in Kasin Sub-Watershed

Well Code	Location	Ground Surface Elevation (m a.s.l.)	Groundwater Level (m a.s.l.)	Depth to Water Table (m bgl)
SM 1	Gading Kasri	440	436.1	3.9
SM 2	Tanjungrejo	478	471.9	6.1
SM 3	Sukun	456	445.6	10.4
SM 4	Bareng	449	434	15
SM 5	Sukun	453	444.6	8.4
SM 6	Kasin	478	475.1	2.9
SM 7	Ciptomulyo	465	462	3
SM 8	Gadang	436	428.2	7.8
SM 9	Bandungrejosari	430	418.5	11.5
SM 10	Kebonsari	429	427.5	1.5

Modeling Results

The groundwater flow and nitrate transport modeling at location was conducted under transient conditions for a simulation period of 3,600 days (approximately 10 years). The initial nitrate concentration was set at 110 ppm in the disposal zone,

representing the point-source contamination input. The flow field showed a dominant groundwater movement from the north toward the south, in line with the local hydraulic gradient. The average groundwater velocity within the aquifer system ranged between 0.25–0.40 m/day, consistent with moderately permeable sandy aquifers. This velocity controlled the advective movement of the contaminant plume over the simulation period.

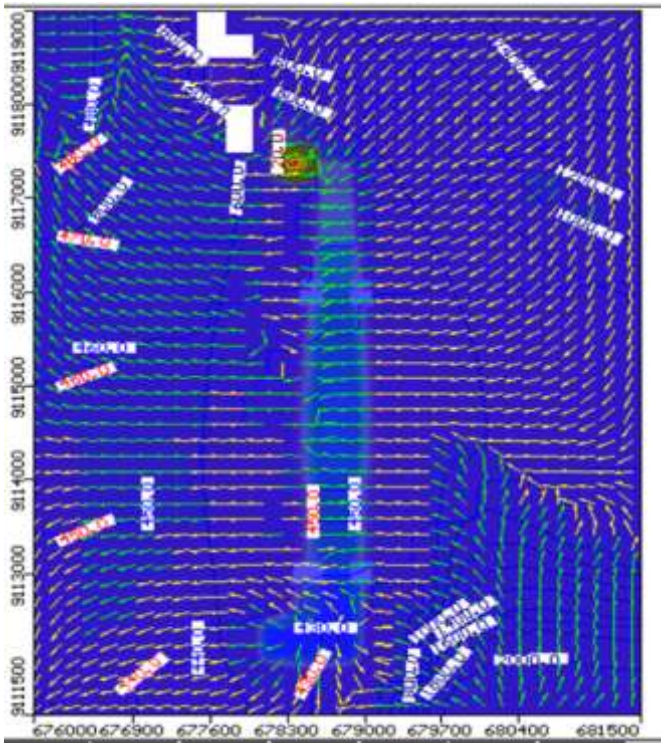

Figure 3. Results of groundwater flow modeling simulation

After 10 years of simulation, the nitrate plume extended horizontally for about 600–700 m from the source zone, while vertically it penetrated to a depth of approximately 25 m. High concentrations exceeding 100 ppm were retained in close proximity to the disposal zone, indicating persistent contamination near the source. At distances of 200–400 m from the source, the nitrate concentration decreased to the range of 40–60 ppm, while at 500–700 m it dropped further to 20–40 ppm due to advection, dispersion, and dilution processes within the aquifer. The elongated plume geometry indicates that horizontal transport was the dominant mechanism, while vertical migration was limited but still significant enough to potentially affect deeper groundwater layers.

These findings are consistent with those reported by Rajaeian et al. (2023), who observed that nitrate plumes in heterogeneous aquifers predominantly spread in the direction of groundwater flow, forming elongated horizontal plumes controlled by advective transport. Similarly, the "*Simulation of Groundwater Contaminant Transport at a Decommissioned Landfill Site – Tainan City, Taiwan*" by Chen et al. (2016) revealed that contaminants from point-source inputs (landfills) remained concentrated near the source for long periods but gradually migrated up to several hundred meters along preferential flow paths. The comparison confirms that in urbanized catchments with high nitrate inputs, plume migration over decadal timescales can substantially degrade groundwater quality in downstream zones, particularly where community wells intersect the preferential flow paths.

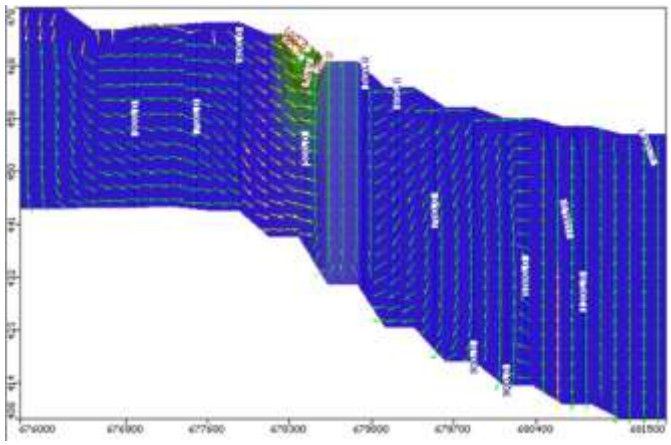

Figure 4. Contaminant Dispersion Patterns

Thus, the modeling at location highlights the long-term persistence and spatial expansion of nitrate contamination under continuous input scenarios, emphasizing the need for integrated groundwater protection measures, such as monitoring networks along predicted plume migration paths and land-use controls in recharge areas.

Conclusion

The transient groundwater flow and nitrate transport simulation using MODFLOW–MT3DMS provided a comprehensive understanding of subsurface dynamics and long-term contaminant migration. With an initial nitrate concentration of 110 ppm, the contaminant plume spread up to ±600–700 m horizontally and reached a depth of ±25 m over 3,600 days (±10 years). The average groundwater velocity of 0.25–0.40 m/day controlled plume migration southward, with high concentrations (>100 ppm) persisting near the source, while concentrations at greater distances decreased to 20–40 ppm due to advection and dispersion. Vertical cross-sections indicated that the contaminant not only spread laterally but also migrated into deeper aquifer layers, influenced by hydraulic pressure differences between strata. In

addition, topographic gradients accelerated migration from higher to lower elevations. Recommended mitigation measures include establishing aquifer protection zones, conducting regular groundwater quality monitoring through observation wells, improving domestic sanitation systems, and applying local control technologies such as reactive barriers. This study highlights the application of numerical modeling to project nitrate movement in a densely populated urban area, thus providing a realistic assessment of risks to community water resources. The main limitations lie in the simplification of aquifer conditions and limited input data, suggesting that future research should incorporate more detailed hydrogeological data, real-time monitoring systems, and multi-contaminant simulations to generate more comprehensive projections.

Acknowledgments
The author would like to thank Dr. Emma Yuliani, ST., MT., Ph.D. for providing the opportunity to participate in this research and for the research funding, as well as Prasetyo Rubiantoro, Amd., SP., M.Ling. for his assistance in data collection for the modeling and for providing research facilities. The author also extends gratitude to the Master Program of Water Resources Engineering, Faculty of Engineering, Universitas Brawijaya, for the academic and institutional support.

Author Contributions
This research article was published thanks to the collaboration between the first author, A. F. M., the second author, E.Y., the third author, A. P. H., and the fourth author, D. V. The authors' contributions to this article include conducting research, analyzing data, and drafting the article. All authors have reviewed the research results and approved the final version of the manuscript.

Funding
This research received no external funding

Conflicts of Interest
The authors declare no conflict of interest.

References

Akiang, F. B., Emujakporue, G. O., & Nwosu, L. I. (2023). Leachate delineation and aquifer vulnerability assessment using geo-electric imaging in a major dumpsite around Calabar Flank, Southern Nigeria. *Environmental Monitoring and Assessment*, *195*(1), 123. https://doi.org/10.1007/s10661-022-10643-2

Alam, S. M. K., Li, P., & Fida, M. (2024). Groundwater Nitrate Pollution Due to Excessive Use of N-Fertilizers in Rural Areas of Bangladesh: Pollution Status, Health Risk, Source Contribution, and Future Impacts. *Exposure and Health*, *16*(1), 159–182. https://doi.org/10.1007/s12403-023-00545-0

Bijay-Singh, & Craswell, E. (2021). Fertilizers and nitrate pollution of surface and ground water: an increasingly pervasive global problem. *SN Applied Sciences*, *3*(4), 518. https://doi.org/10.1007/s42452-021-04521-8

Chen, C.-S., Tu, C.-H., Chen, S.-J., & Chen, C.-C. (2016). Simulation of Groundwater Contaminant Transport at a Decommissioned Landfill Site—A Case Study, Tainan City, Taiwan. *International Journal of Environmental Research and Public Health*, *13*(5), 467. https://doi.org/10.3390/ijerph13050467

Eluwole, A. B., OlaOlorun, O. A., Ademilua, O. L., Talabi, A. O., Aturamu, A. O., Ajisafe, Y. C., Ojo, O. F., & Ajayi, C. A. (2020). Subsurface electrical resistivity modelling over a suspected fault zone at Ojirami, Southwestern Nigeria. *Modeling Earth Systems and Environment*, *6*(4), 2543–2551. https://doi.org/10.1007/s40808-020-00848-0

Eze, S. U., Abolarin, M. O., Ozegin, K. O., Bello, M. A., & William, S. J. (2022). Numerical modeling of 2-D and 3-D geoelectrical resistivity data for engineering site investigation and groundwater flow direction study in a sedimentary terrain. *Modeling Earth Systems and Environment*, *8*(3), 3737–3755. https://doi.org/10.1007/s40808-021-01325-y

Foster, S. (2022). The key role for groundwater in urban water-supply security. *Journal of Water and Climate Change*, *13*(10), 3566–3577. https://doi.org/10.2166/wcc.2022.174

Ibrahim, D., Nemoto, T., & Raghavan, V. (2025). Hydrogeophysical Analysis of Vertical Electrical Soundings for Groundwater Potential and Aquifer Vulnerability Evaluation in the Federal Capital Territory, Abuja, Nigeria. *International Journal of Geoinformatics*, *21*(1), 97–110. https://doi.org/10.52939/ijg.v21i1.3803

Jabeen, M., Ahmad, Z., & Ashraf, A. (2019). Monitoring regional groundwater flow and contaminant transport in Southern Punjab, Pakistan, using numerical modeling approach. *Arabian Journal of Geosciences*, *12*(18), 570. https://doi.org/10.1007/s12517-019-4766-5

Kuroda, K., & Fukushi, T. (2009). Groundwater Contamination in Urban Areas. *Jurnal Teknik Lingkungan*, *23*(1), 125–149. https://doi.org/10.1007/978-4-431-78399-2_7

Laoufi, A., Boudjema, A., Guettaia, S., Derdour, A., & Almaliki, A. H. (2024). Integrated Simulation of Groundwater Flow and Nitrate Transport in an Alluvial Aquifer Using MODFLOW and MT3D: Insights into Pollution Dynamics and Management Strategies. *Sustainability*, *16*(23), 10777. https://doi.org/10.3390/su162310777

Mulyadi, D., & Rosadi, P. E. (2022). Pemodelan Air Tanah Pada Tambang Terbuka Andesit Di Desa Dadirejo, Kecamatan Bagelen, Kabupaten Purworejo, Provinsi Jawa Tengah. *Jurnal Inovasi Pertambangan Dan Lingkungan*, *1*(2), 59–70. https://doi.org/10.15408/jipl.v1i2.22761

Prayogo, T. B., Bisri, M., Fadhia, K. F., & Martius, A. F. (2024). Aquifer potential investigation applying vertical electrical sounding in Bango sub-catchment area. *IOP Conference Series: Earth and Environmental Science*, *1311*(1), 012038. https://doi.org/10.1088/1755-1315/1311/1/012038

Priyan, K. (2021). Issues and Challenges of Groundwater and Surface Water Management in Semi-Arid Regions. In *Groundwater Resources Development and Planning in the Semi-Arid Region* (pp. 1–17). Springer International Publishing. https://doi.org/10.1007/978-3-030-68124-1_1

Rajaeian, S., Ketabchi, H., & Ebadi, T. (2023). Investigation on quantitative and qualitative changes of groundwater resources using MODFLOW and MT3DMS: a case study of Hashtgerd aquifer, Iran. *Environment, Development and Sustainability*, *26*(2), 4679–4704. https://doi.org/10.1007/s10668-022-02904-4

Rashmi, I., Roy, T., Kartika, K. S., Pal, R., Coumar, V., Kala, S., & Shinoji, K. C. (2020). Organic and Inorganic Fertilizer Contaminants in Agriculture: Impact on Soil and Water Resources. In *Contaminants in Agriculture* (pp. 3–41). Springer International Publishing. https://doi.org/10.1007/978-3-030-41552-5_1

Rasool, U., Chen, J., Muhammad, S., Siddique, J., Venkatramanan, S., Sabarathinam, C., Siddique, M. A., & Rasool, M. A. (2020). Geoinformatics and geophysical survey-based estimation of best groundwater potential sites through surface and subsurface indicators. *Arabian Journal of Geosciences*, *13*(15), 702. https://doi.org/10.1007/s12517-020-05496-3

Samborska-Goik, K., & Pogrzeba, M. (2024). A Critical Review of the Modelling Tools for the Reactive Transport of Organic Contaminants. *Applied Sciences*, *14*(9), 3675. https://doi.org/10.3390/app14093675

Shakeri, R., Nassery, H. R., & Ebadi, T. (2023). Numerical modeling of groundwater flow and nitrate transport using MODFLOW and MT3DMS in the Karaj alluvial aquifer, Iran. *Environmental Monitoring and Assessment*, *195*(1), 242. https://doi.org/10.1007/s10661-022-10881-4

Zheng, C., & Wang, P. P. (1999). An integrated global and local optimization approach for remediation system design. *Water Resources Research*, *35*(1), 137–148. https://doi.org/10.1029/1998WR900032